Proceedings of the Mustansiriyah International Conference on Applied Physics (MICAP-2021)

Modified Hydrothermal Preparation of ZnO/NiO Nano-Heterojunction for Enhancement of Photocatalytic Activity

Sahar M. Ali*, Osama A.A. Dakhil and Emad H. Hussein

Department of Physics, College of Science, Mustansiriyah University, Baghdad, Iraq

Doi: 10.12693/APhysPolA.140.327 *e-mail: saharmohamed@uomustansiriyah.edu.iq

Fabrication of zinc oxide/nickel oxide (ZnO/NiO) nano-heterojunction films on glass substrates using hydrothermal and modified hydrothermal techniques was investigated. Various tools were employed for the evaluation of the structural nature and to determine the optical properties of the heterojunction. Besides, the photoactivity of the heterostructures was observed under the influence of the prepared films on the degradation of methylene blue (MB) dye. According to the X-ray diffraction and scanning electron microscopic images, the hydrothermal technique resulted in hexagonal-phase nanoplates with a thickness of 45.0–74.0 nm and nano-spherical particles of diameters of 60.6–88.0 nm. In contrast, the modified hydrothermal technique showed nanosheets of 29.0–38.0 nm thick. The photodegradation efficiency of the films was found to be strongly enhanced and reached 93% using the modified hydrothermal film. The prepared heterostructures are affordable and applicable for the degradation of contaminants in water.

topics: hydrothermal technique, modified hydrothermal technique, ZnO/NiO heterojunction, photocatalytic activity

1. Introduction

Metal oxide materials are widely used in modern technology. Gas sensing, surface acoustic waves, and photocatalysts are such applications. ZnO has been confirmed to be an effective photocatalyst for removing several organic contaminants from water due to good properties such as strong oxidant and nontoxicity [1–3]. It can absorb ultraviolet (UV) light in the range of its energy gap (3.37 eV), and hence, it shows good photocatalytic activity for the solar radiation [4, 5].

Nickel oxide (NiO) as a wide bandgap *p*-type semiconductor has confirmed its advantages for photocatalytic activity [6–8]. Hence by involving two nano-powder semiconductors, organic and inorganic contaminants spread in water [9, 10] can be oxidized. Charge separation is simply achieved when two different energy gap materials are connected. The hetero-nanostructures of SnO_2/ZnO [11] NiO/ZnO [12] and TiO_2/NiO [13] have already been used for high photocatalytic activity.

ZnO was synthesized by various techniques like pulsed-laser ablation, chemical-bath deposition, hydrothermal, and electrospun [14–18]. In this work, a comparison between the traditional and modified hydrothermal routes was conducted. The influence of technique type on the structures and photocatalytic behavior of ZnO/NiO was studied.

2. Materials and method

The materials used in experiments included: 98.5% zinc nitrate hexahydrate ($Zn(NO_3)_2 \cdot 6H_2O$, Scharlau, Spain), 99% nickel nitrate hexahydrate ($Ni(NO_3)_2 \cdot 6H_2O$) and 99% hexamethylenetetramine (HMT, $C_6H1_2N_4$, Hi-media India). Methylene blue (MB) dye from Sigma-Aldrich, Germany was used as the contaminant.

2.1. Characterization

The structures of the films were studied using the $\theta/2\theta$ scans of X-ray diffraction (XRD) by PIXcel diffractometer within the range of 20–80°. The morphologies of the films were evaluated by Zeiss SIGMA VP-Field-emission scanning electron microscopy (FE-SEM). The absorption and photoactivity measurements were recorded within a wavelength range between 200 and 900 nm using a spectrophotometer of Double Beam Li-2800.

2.2. Synthesis of ZnO/NiO heterojunction

Substrates in the form of 2×2 cm^2 glass slides were immersed ultrasonically in ethanol for 15 min and washed in distilled water (DW). A thin gold (Au) seed layer was sputtered on the substrates by a GSL-1100X-SPC 16-3, MTI Corporation DC-Sputtering System at a 0.25 mbar for one minute. Then, the substrate was heated at 500° for 2 h.

2.3. Hydrothermal technique of obtaining ZnO/NiO (HT-ZN)

At the initial stage of the experiment, $Zn(NO_3)_2 \cdot 6H_2O$, HMT, and $Ni(NO_3)_2 \cdot 6H_2O$ of concentrations as 0.02 M + 0.02 M + 0.01 M were mixed in DW (80 ml) with a 10 min stirring until pH reached 6. And, M is mole per liter. The substrate was submerged in the prepared solution inside an autoclave at 90°C. After 3 h, the substrate was cleaned with DW, and dried at 60°C on a hotplate for 10 min. The prepared structure of ZnO/NiO was subject to thermal annealing at 400°C for 1 h.

2.4. Modified-hydrothermal technique of obtaining ZnO/NiO (MHT-ZN)

The modified-hydrothermal technique of ZnO/NiO (MHT-ZN) involved two steps. Firstly, it consisted in dissolving Zn $(NO_3)_2 \cdot 6H_2O$ and HMT of concentrations 0.02 M + 0.02 M in DW (80 ml) with stirring for 10 min and was followed by the same order of HT-ZN to get a ZnO layer. Secondly, the ZnO layer was immersed in a mixture of $Ni(NO_3)_2 \cdot 6H_2O$ (0.01 M) and HMT (0.01 M) using the same conditions of deposition, and then it was treated thermally at 400° for 1 h to improve the crystal quality of the ZnO/NiO film.

2.5. Photoactivity tests

Measurement of degradation was carried out by the MB dye dissolved in DW. The films were submerged in the solution for 30 min in dark to let the accumulation of contaminants on the film. First, the optical absorption was recorded in the darkness. Then, the films was exposed to the sunlight and measured for 30 min each. To determine the degradation efficiency (P), we used

$$P = \frac{C_0 - C_t}{C_0} \times 100\% \quad (1)$$

where C_0 and C_t are the dye concentrations [mg/L], initial and final, respectively. The value $C_0 = 10$ mg/L was chosen. The absorption spectra of MB were determined at 665 nm.

3. Results and discussion

3.1. Morphology of ZnO/NiO

The morphologies of the films are shown in Fig. 1. In the HT-ZN method, hexagonal nanoplates with thickness of 45–74 nm and nano-spherical particles of diameters of 60–87 nm are seen (Fig. 1a and b). In the MHT-ZN technique, nanosheets of thickness of 29–37 nm are observed (Fig. 1d and e). Figure 1c and f shows that the thickness of the HT-ZN and MHT-ZN films are 420 nm and 714.0 nm, respectively.

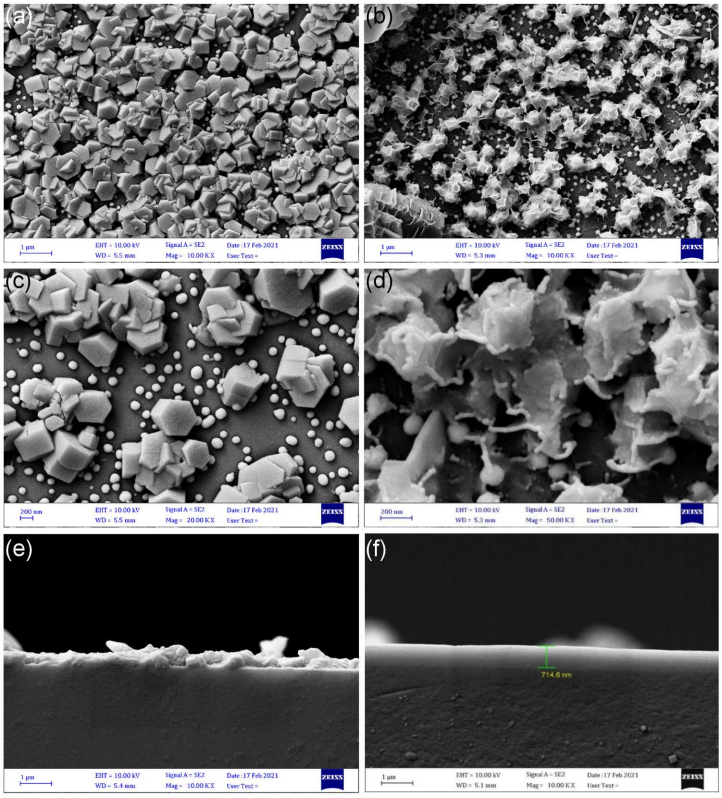

Fig. 1. FESEM images of ZnO/NiO heterojunction by (a, c) the hydrothermal technique, (b, d) the modified-hydrothermal technique, (e) the cross-section of hydrothermal, and (f) the cross-section of modified-hydrothermal technique.

4. XRD measurements

Figure 2 illustrates the XRD patterns of the fabricated ZnO/NiO structures. As shown in Fig. 2a, peaks of the HT-ZN technique structures are present at 31.77° (100), 34.438° (002), 36.253° (101), 47.55° (102), 56.602° (110), 66.38° (200), 67.96° (112), and 69.12° (201), suggesting the hexagonal structure of the ZnO nanostructures as referred by the standard JCPDS (76-0704) card. There are two sharp peaks of (100) and (101) planes which are considered the preferable orientation of the nanostructures [19]. The other peaks seen at 38.19° (101) and 62.87° (110) are due to the cubic structure of the NiO nanoparticles according to the reference JCPDS (44-1159).

Figure 2b shows the XRD pattern of the MHT-ZN technique in which the peaks observed at 31.79° (100), 34.46° (002), 36.29° (101), 47.6° (102), 56.65° (110), and 69.16° (201) are indexed to the ZnO hexagonal structure. Also, the peaks at 38.26° (101), 42.94° (012), and 62.8° (110) confirm the cubic structure of NiO. The remaining peaks seen at 44.4° (002) and 64.65° (220) are the diffraction peaks of the gold seeds.

The average crystallite size (D) was calculated at the Bragg angle (θ) by applying an X-ray of wavelength of $\lambda = 1.5408$, and using the Debye–Scherrer equation

$$D = \frac{0.9\lambda}{\beta \cos(\theta)}, \tag{2}$$

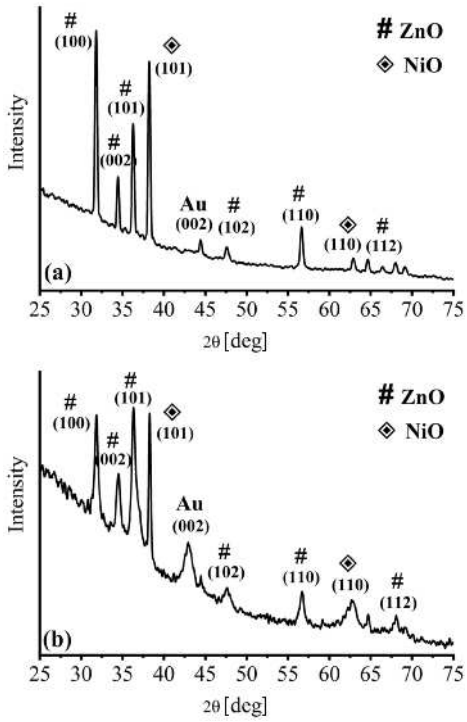

Fig. 2. XRD curves of the ZnO/ NiO film fabricated by (a) hydrothermal and (b) modified-hydrothermal method at 90° for 3 h'.

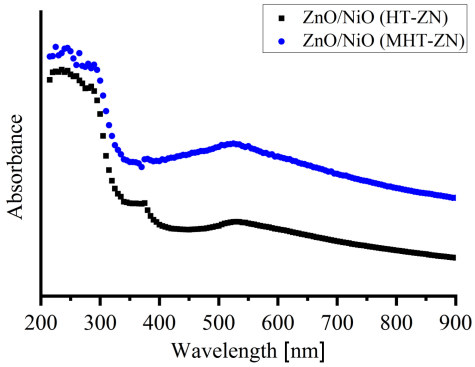

Fig. 3. The HT and MHT ZnO/NiO absorption spectra.

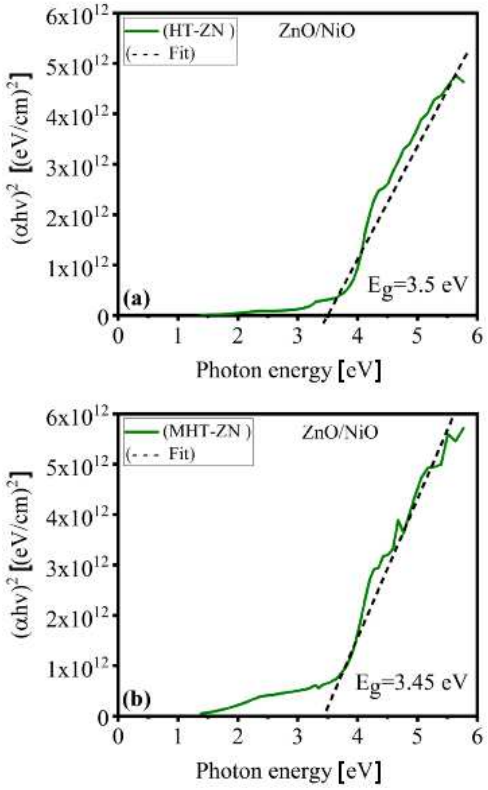

Fig. 4. The direct bandgaps of ZnO/NiO fabricated by (a) HT and (b) MHT method.

where β is the full-width half maximum. The average crystallite sizes of the ZnO/NiO HT-ZN and the MHT-ZN films were calculated to be 40.81 nm and 18.15 nm, respectively, at the (101) plane.

4.1. UV–VIS spectroscopy

The absorption spectra of both heterostructure types recorded in the wavelength range of 200–900 nm are shown in Fig. 3.

The estimated bandgaps of the HT-ZN and MHT-ZN films are 3.5 eV and 3.45 eV, as shown in Fig. 4. The shifts of the standard values in the energy gap could be caused by strain in the crystal [20] or the quantum size effect [21].

4.2. Photoactivity measurements

The photoactivity measurements of both samples are illustrated in Fig. 5. The efficiency of nanostructures for the MB degradation is dependent of the fabrication technique. The decomposition efficacy of the HT-ZN film under light subject is equal to 88% which increases to 93% by the MHT-ZN technique.

When the energy bands of ZnO and NiO are aligned in a p–n junction, electrons from the valence band move to the conduction band will leave holes behind by activating the junction. Also, the charges continue to transfer between the regions of the junction until equilibrium is reached. As the lifetime of the charge carriers increases due to the separation, the decomposition efficiency is possibly enhanced at the solid–liquid interface [22]. Besides, the photoelectrons separated from holes can reduce the charge recombination. These photoelectrons that are accumulated on the NiO surface can adsorb O_2, thus generating O_2^-. In another reaction, the holes accumulated on the ZnO move to H_2O and OH^- generating OH groups [23]. The mechanism of charge transfer between both p–n junction sides is depicted in Fig. 6. However, the photocatalytic efficiency has already been enhanced by NiO/ZnO heterojunction due to larger number of photo-generating electrons and holes [24–28].

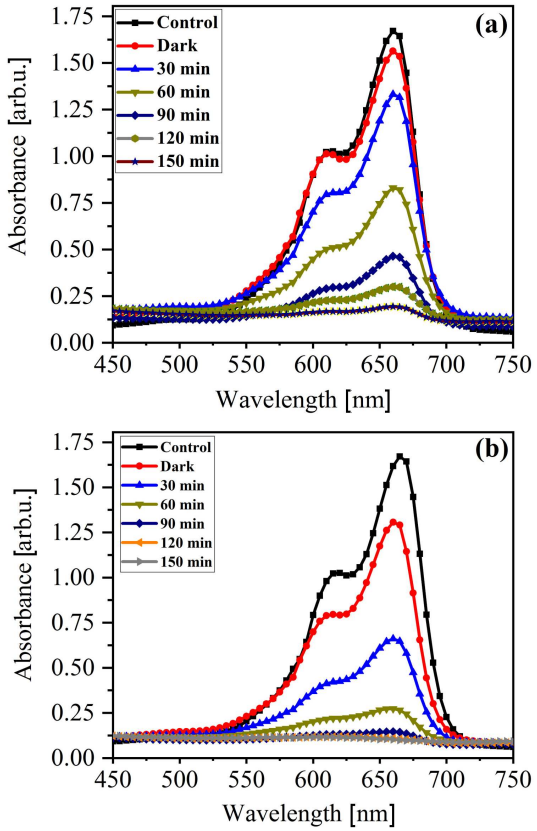

Fig. 5. UV–VIS photodegradation of MB subject to the sunlight by (a) hydrothermal and (b) modified-hydrothermal routes.

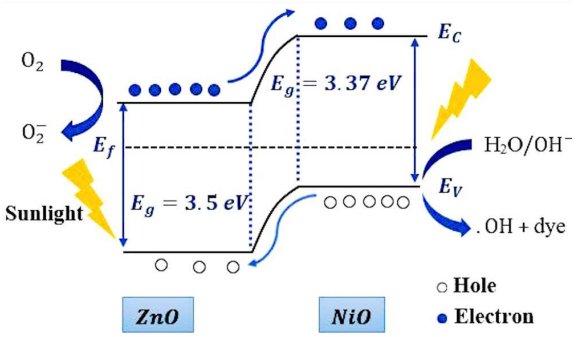

Fig. 6. Schematic illustration of photocatalytic degradation of MB dye.

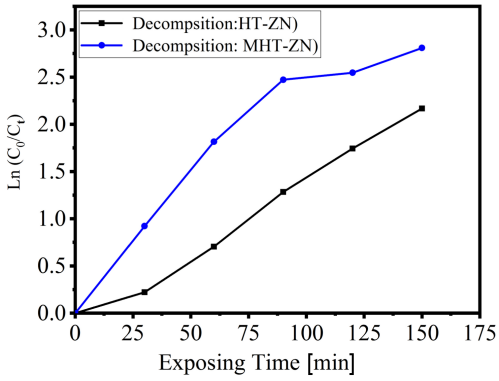

Fig. 7. The first-order kinetics of the ZnO/NiO films against methylene blue dye under sunlight.

The reaction rate equation given below provides the relationship between $\ln(C_0/C_t)$ and exposing time t by which one can calculate the pseudo-first-order rate constant k. This relation is given by

$$\ln\left(\frac{C_0}{C_t}\right) = kt. \tag{3}$$

As Fig. 7 shows, the values of k calculated for the HT-ZN and MHT-ZN films are found to be 0.01445/min and 0.01865/min, respectively, confirming the dependence of the photodegradation efficiency on the fabrication technique.

5. Conclusions

ZnO/NiO heterojunction was fabricated using traditional and modified-hydrothermal techniques. The obtained morphology of ZnO/NiO p–n junctions was different in each technique. In the hydrothermal technique, the hexagonal nanoplates and nano-spherical particles were obtained. In contrast, the modified-hydrothermal technique resulted in nanosheets. Furthermore, the photodegradation efficiency using the MB dye was enhanced to 93% by the modified technique. The results confirm high possibility of ZnO/NiO heterojunctions for water treatment.

Acknowledgments

The authors thanks and appreciations are due to the support submitted by the Department of Physics, College of Science at Mustansiriyah University, Baghdad, Iraq (see uomustansiriyah.edu.iq/).

References

[1] L. Li, W. Wang, H. Liu, X. Liu, Q. Song, S. Ren, *J. Phys. Chem. C* **113**, 8460 (2009).

[2] T. Alammar, A.-V. Mudring, *Mater. Lett.* **63**, 732 (2009).

[3] S. Tarish, Z. Wang, A. Al-Haddad, C. Wang, A. Ispas, H. Romanus, P. Schaaf, Y. Lei, *J. Phys. Chem. C* **119**, 1575 (2015).

[4] C. Tian, Q. Zhang, A. Wu, M. Jiang, Z. Liang, B. Jiang, H. Fu, *Chem. Commun.* **48**, 2858 (2012).

[5] L. Yansheng, J. Zhenhua, Y. Nan, G. Hong, *J. Environ. Sci.* **21**, S69 (2009).

[6] G. Boschloo A. Hagfeldt, *J. Phys. Chem. B* **105**, 3039 (2001).

[7] F.A. Harraz, R.M. Mohamed, A. Shawky, I.A. Ibrahim, *J. Alloy Compd.* **508**, 133 (2010).

[8] M.M. Jasim, O.A.A. Dakhil, E.H. Hussein, H.I. Abdullah, *J. Mater. Sci. Mater. Electron.* **31**, 10707 (2020).

[9] A. Mills, S. Le Hunte, *J. Photochem. Photobiol. A Chem.* **108**, 1 (1997).

[10] M. Hara, H. Hasei, M. Yashima, S. Ikeda, T. Takata, J.N. Kondo, K. Domen, *Appl. Catal. A General.* **190**, 35 (2000).

[11] L. Zheng, Y. Zheng, C. Chen, Y. Zhan, X. Lin, Q. Zheng, K. Wei, J. Zhu, *Inorg. Chem.* **48**, 1819 (2009).

[12] A. Hameed, T. Montini, V. Gombac, P. Fornasiero, *Photochem. Photobiol. Sci.* **8**, 677 (2009).

[13] R. Vinoth, P. Karthik, K. Devan, B. Neppolian, M. Ashokkumar, *Ultrason. Sonochem.* **35**, 655 (2017).

[14] K. N. Abbas, N. Bidin, R.S. Sabry, *Ceram. Int.* **42**, 13535 (2016).

[15] S. M. Ali, E.H. Hussein, O.A.A. Dakhil, *Nano Futures* **5**, 035001 (2021).

[16] R. Yumiyama, D. Hyakutake, M. Hagiwara, E. Hosono, H. Matsuda, S. Fujihara, *CrystEngComm* **22**, 2447 (2020).

[17] K.N. Abbas, R.S. Sabry, R.A. Alkareem, E.H. Hussein, S. Islam, N. Bidin, A.M. Abbas, *J. Aust. Ceram. Soc.* **56**, 1377 (2020).

[18] G. Panthi, M. Park, H.-Y. Kim, S.-Y. Lee, S.-J. Park, *J. Ind. Eng. Chem.* **21**, 26 (2015).

[19] Z. Lin Wang, *J. Phys. Condens. Matter* **16**, R829 (2004).

[20] F.G. Hone, F.K. Ampong, *Mater. Chem. Phys.* **183**, 320 (2016).

[21] D. Nunes, A. Pimentel, A. Gonçalves, S. Pereira, R. Branquinho, P. Barquinha, E. Fortunato, R. Martins, *Sci. Technol.* **34**, 043001 (2019).

[22] Z. Zhang, C. Shao, X. Li, C. Wang, M. Zhang, Y. Liu, *ACS Appl. Mater. Interfaces* **2**, 2915 (2010).

[23] C. Luo, D. Li, W. Wu, Y. Zhang, C. Pan, *RSC Adv.* **4**, 3090 (2014).

[24] M. Xiao, Y. Lu, Y. Li, H. Song, L. Zhu, Z. Ye, *RSC Adv.* **4**, 34649 (2014).

[25] U.S.U. Thampy, A. Mahesh, K. S. Sibi, I.N. Jawahar, V. Biju, *SN Appl. Sci.* **1**, 1478 (2019).

[26] S. Chu, H. Li, Y. Wang, Q. Ma, H. Li, Q. Zhang, P. Yang, *Mater. Lett.* **252**, 219 (2019).

[27] S.M. Aydoghmish, S.A.H. Tabrizi, A.S. Teluri, *Ceram. Int.* **45**, 14934 (2019).

[28] S. Yousaf, S. Zulfiqar, M.I. Din, P.O. Agboola, M.F. Aly Aboud, M. Farooq Warsi, I. Shakir, *J. Mater. Res. Technol.* **12**, 999 (2021).